JCI insight

Selective CAR-T cell mediated B cell depletion suppresses interferon signature in SLE

Artur Wilhelm, … , Georg Schett, Gerhard Krönke

JCI Insight. 2024. https://doi.org/10.1172/jci.insight.179433.

Resource and Technical Advance In-Press Preview **Immunology**

Applying advanced molecular profiling together with highly specific targeted therapies offers the possibility to better dissect the mechanisms underlying immune mediated inflammatory diseases such as systemic lupus erythematosus (SLE) in humans. Here we apply a combination of single cell RNA sequencing and T/B cell repertoire analysis to perform an in-depth characterization of molecular changes in the immune-signature upon CD19 CAR T cell-mediated depletion of B cells in SLE patients. The resulting datasets do not only confirm a selective CAR T cell-mediated reset of the B cell response, but simultaneously reveal consequent changes in the transcriptional signature of monocyte and T cell subsets that respond with a profound reduction in type 1 interferon signaling. Our current data thus provide evidence for a causal relationship between the B cell response and the increased interferon signature observed in SLE and additionally demonstrate the usefulness of combining targeted therapies and novel analytic approaches to decipher molecular mechanisms of immune-mediated inflammatory diseases in humans.

Selective CAR-T cell mediated B cell depletion suppresses interferon signature in SLE

Artur Wilhelm[1,2]*, David Chambers[1,2]*, Fabian Müller[2,3], Aline Bozec[1,2], Ricardo Grieshaber-Bouyer[1,2], Thomas Winkler[4], Dimitrios Mougiakakos[5], Andreas Mackensen[2,3], Georg Schett[1,2]*, Gerhard Krönke[1,2,6]*

[1]Department of Internal Medicine 3 - Rheumatology and Immunology, FAU Erlangen-Nürnberg and Universitätsklinikum Erlangen, Erlangen, Germany; [2]Deutsches Zentrum Immuntherapie, Universitätsklinikum Erlangen, Friedrich-Alexander University (FAU) Erlangen- Nürnberg, Erlangen, Germany; [3]Department of Internal Medicine 5 – Hematology and Oncology, FAU Erlangen-Nürnberg and Universitätsklinikum Erlangen, Erlangen, Germany; [4]Department of Genetics, Friedrich-Alexander University (FAU) Erlangen-Nürnberg, Erlangen, Germany; [5]Department of Hematology and Oncology, Otto-von-Guericke University Magdeburg, Magdeburg, Germany; [6]Department of Rheumatology and Clinical Immunology, Charité, Unversitätsmedizin Berlin, Berlin, Germany.

*Equally contributed

Correspondence to: Gerhard Krönke, E-mail: Gerhard.kroenke@charite.de

Abstract

Applying advanced molecular profiling together with highly specific targeted therapies offers the possibility to better dissect the mechanisms underlying immune mediated inflammatory diseases such as systemic lupus erythematosus (SLE) in humans. Here we apply a combination of single cell RNA sequencing and T/B cell repertoire analysis to perform an in-depth characterization of molecular changes in the immune-signature upon CD19 CAR T cell-mediated depletion of B cells in SLE patients. The resulting datasets do not only confirm a selective CAR T cell-mediated reset of the B cell response, but simultaneously reveal consequent changes in the transcriptional signature of monocyte and T cell subsets that respond with a profound reduction in type 1 interferon signaling. Our current data thus provide evidence for a causal relationship between the B cell response and the increased interferon signature observed in SLE and additionally demonstrate the usefulness of combining targeted therapies and novel analytic approaches to decipher molecular mechanisms of immune-mediated inflammatory diseases in humans.

Introduction

Systemic Lupus Erythematosus (SLE) represents a prototypic autoimmune disease characterized by chronic inflammation and progressive inflammation-associated tissue damage of multiple organs including kidneys, joints and skin (1). SLE is considered to result from a break in systemic immune tolerance with SLE patients displaying autoantibodies against ubiquitous nuclear antigens such as double-stranded DNA and histones (2). B cells seem to exert a pivotal role during the pathogenesis of SLE where they are considered to act as precursors of autoantibody producing plasmablasts and plasma cells and additionally provide the base of a pathogenic immune memory in form of autoreactive memory B cells that are able to sustain persistent autoimmunity (3).

Another hallmark of SLE is the presence of an increased type 1 interferon signature in form of an enhanced expression of multiple interferon-inducible genes in peripheral blood mononuclear cells (PBMCs) indicating an additional key role of interferons in the development of SLE (4-6). In accordance, also a range of genetic disorders, which result in increased type 1 interferon production or the treatment with recombinant type 1 interferons themselves can trigger onset of an SLE-like disease pathology (7, 8). Blockade of the type 1 interferon receptor has consequently emerged as an effective therapy for a subset of SLE patients (9).

Together, these findings have provoked important questions not only about the cellular sources and targets of type 1 interferons, but also about the triggers and the causative series of events that eventually foster interferon production and B cell activation, respectively, in SLE patients.

Previous clinical trials in SLE patients studying B cell depletion yielded discrepant results (10), which were partially due to the inefficient depletion of tissue B cells in response to

therapeutic CD20 antibodies (11). Meanwhile, CD19 CAR T cells have emerged as a novel therapeutic tool that has demonstrated superiority to antibody-mediated B cell depletion during the therapy of B cell lymphomas and B cell leukemias (12). Increasing evidence indicates that CD19 CAR T cell therapy also enables a profound depletion of B cells in SLE patients and patients suffering from other types of B cell-mediated autoimmune disease, an approach that was able to facilitate a sustained and drug-free remission in such patients (13-16). Studying the molecular and cellular effects of a CD19 CAR T cell-mediated elimination of B cells in SLE patients thus provides a unique opportunity to directly learn from precision medicine and better understand the contribution of B cells to the pathogenesis of SLE as part of a reverse translational approach.

In the current manuscript, we provide data on the molecular role of B cells in SLE that are based on single cell RNA sequencing (scRNAseq) of PBMCs as well as a repertoire analysis of B cell and T cell receptors in SLE patients before and after CD19 CAR T cell therapy. The insights derived from this analysis do not only support a CD19 CAR T cell-mediated reset of the memory B cell compartment, but also the parallel inhibition of the interferon signature in monocytes and T cells of SLE patients. CD19 CAR T cell therapy as precision medicine approach in conjunction with deep molecular phenotyping thus provide support for the central role of autoreactive B cells during the pathogenesis of SLE as well as for the B cell-dependent increase in type 1 interferon signaling previously observed in PBMCs of SLE patients.

Results

We conducted a scRNAseq-based analysis of PBMCs derived from a cohort of SLE patients (Table S1) before and after a therapy with CD19 CAR T cells. The analysis post-CD19 CAR T

cell treatment was performed at a stage when, after initial depletion, de-novo B cells had already repopulated the peripheral blood. Numbers of peripheral blood B cells were monitored and B cell repopulation was observed in the individual patients between 9 and 28 weeks after CD19 CAR T cell treatment (Table S2). This approach thus enabled us to study the global impact of a defined CD19 CAR T cell-mediated depletion of B cells on the immune status of SLE patients and to consequently understand the precise contribution of B cell (auto-)reactivity to the molecular immune pathogenesis of SLE. Recent data showed a profound clinical and serological response of these patients, which entered a drug-free remission with normalization of clinical disease activity parameters and a reduction or disappearance of autoantibodies despite the repopulation of B cells (16). These findings are thus suggestive of a deep reset of autoimmunity in response to CD19 CAR-T cell therapy in this cohort of SLE patients (14, 16).

Our current scRNAseq analysis showed that, apart from an initial depletion of B cells, CD19 CAR T cell treatment did not provoke major changes in the basic cellular composition of T cells and monocytes at a stage when de novo B cells had repopulated the peripheral blood (Fig. 1A-C). To understand enduring molecular consequences of a singular CD19 CAR T cell-mediated reset of the B cell response, we subsequently performed a pathway enrichment analysis based on changes in gene expression of total PBMCs in response to therapy (Fig. 1D and Fig. 1E). Notably, interferon (IFN) signaling in general, and type 1 IFN (IFN alpha/beta) signaling in particular, emerged as the major pathways that were decreased in response to CD19 CAR T cell treatment. We accordingly observed a significant reduction in the expression of a large set of IFN-induced genes such as *IRF7* or *ISG15* that, prior to CD19 CAR T cell therapy, were primarily expressed within monocyte and T cell subsets of this cohort of SLE patients (Fig. 1F and Fig. 1G).

A more detailed analysis of the molecular signature of individual T cell subsets within the peripheral blood did not reveal major changes in the frequency of $CD4^+$ and $CD8^+$ T cells as well as of regulatory T cells in response to CD19 CAR T cell therapy (Fig. 2A-C). Analysis of differential gene expression changes as well as pathway enrichment analyses, specifically performed within the T cell dataset, again identified IFN signaling as the top regulated pathway and different IFN-induced genes that were downregulated in SLE patients upon CD19 CAR T cell therapy in different T cell subsets (Fig. 2D-F). Repertoire analysis showed that CD19 CAR T cell therapy did not affect the T cell receptor (TCR) repertoire with T cells maintaining a stable distribution in the expression of TCR-β chains before and after treatment (Fig. 2G). We additionally performed an optimized likelihood estimate analysis to compute the generation probability of detected CDR3 sequences within the sequenced TCRs (Fig. 2G). This approach showed that the calculated generation probabilities for both TCRα and TCRβ chains did not differ before and after CD19 CAR T cell therapy, indicating that the T cell repertoire remained unaffected in response to this therapeutic approach. Among the datasets obtained post B cell reconstitution, we could not detect CAR T cells.

Finally, we analyzed the scRNAseq-based gene expression profile and repertoire of B cells prior and past CD19 CAR-T cell treatment after B cell reconstitution. This approach showed a substantial reduction of memory B cells as well as a parallel expansion of transitional and transitional/immature B cells upon the CAR T cell-induced reset of the B cell compartment (Fig. 3A-C). In accordance with an early and/or intermediate developmental stage of reconstituted B cells, we observed an enhanced expression of genes such as *PLD4* in this cellular compartment when studying differential gene expression in B cells before and after CAR T cell therapy (Fig. 3D). Pathway enrichment analysis accordingly showed that the

pathways, which changed upon repopulation of B cells in response to CD19 CAR T cell treatment, were mostly associated with BCR and FcγR signaling (Fig. 3E and Fig. 3F).

In accordance with the shift in B cell subpopulations and the reduction of memory B cells, we observed a virtual disappearance of IgG- and IgA- expressing B cells, while IgM- and IgD-expressing B cell clones expanded (Fig. 4A), which was in accordance with our previously published data (14, 16). B cells that repopulated after CD19 CAR T cell treatment additionally displayed an increase in the generation probability of their currently expressed immunoglobulin chains, which was in line with a naïve and unexperienced repertoire and consistent with a reset of the B cell memory compartment (Fig. 4A).

We additionally performed a characterization of B cell clones that displayed an expansion prior and after CD19 CAR T cell treatment, respectively. Here we identified several expanded IgG- and IgA-expressing clones that disappeared in response to CD19 CAR T cells, whereas clones that expanded after therapy exclusively showed expression of IgM or IgD (Fig. 4B and Fig. 4C).

Discussion

SLE represents a heterogenous spectrum of systemic autoimmune diseases that share common denominators. Apart from SLE-typical clinical features, SLE patients display an increased activation and autoreactivity within the B cell and plasma cell compartments (3), the presence of antinuclear antibodies (2) as well as an elevated type 1 interferon signature (5). Although these findings have resulted in the development of various targeted therapeutic approaches such as depletion of B cells or blockade of interferon signaling, we lack a full understanding of the molecular base of this disease and of the series of events that trigger the observed break in self-tolerance or onset of SLE (17). Targeted therapies

such as monoclonal antibodies and CAR T cells do not only offer promising therapeutic tools, but simultaneously allow a reverse translational approach that enables us to better understand the underlying disease itself and thereby identify novel therapeutic targets and treatment strategies.

Our current data show that a CD19 CAR T cell-based therapy serves as effective strategy to selectively reset the B cell compartment without affecting the composition of other immune cell subsets or the nature of the T cell response. The overall composition of monocytes, dendritic cells and T cell subsets as well as the TCR repertoire remained largely unaltered, whereas we observed profound changes in the distribution of B cell subsets, the B cell receptor repertoire and the B cell-dependent immune memory in response to this treatment strategy. Formally, we cannot exclude that the lymphotoxic conditioning therapy with fludarabine and cyclophosphamide, which is given prior to CAR T cell therapy, contributes to the beneficial effects observed in this cohort of SLE patients. The selective reset of the B cell response, however, suggests that the therapeutic effect is primarily linked to the action of CD19 CAR T cells.

Notably, our data show that CD19 CAR T cell therapy is highly effective in eliminating IgG^+ and IgA^+ memory B cells, which fail to repopulate the peripheral blood despite the reappearance of other B cell subsets following CD19 CAR T cell treatment. This finding provides a potential explanation for the clinical efficacy of this therapeutic approach as persistence and/or reappearance of memory B cells upon CD20 antibody-mediated B cell depletion have been previously associated with treatment failures and disease relapses (18, 19). In the future, it will be important to directly assess potential differences in the molecular signature of repopulating B cells in response to different B cell-depleting strategies such as CD19 CAR T cells and CD20 antibodies, respectively.

The major CD19 CAR T cell-induced change observed in PBMCs others than B cells was a profound reduction in the type 1 IFN signature in monocytes and T cells. These finding clearly indicates that the aberrant B cell response in SLE (directly or indirectly) triggers the enhanced IFN signature observed in PBMCs of SLE patients and suggests that the increase in type 1 IFN signaling is a consequence rather than a cause of the increased activation of autoreactive B cells in SLE. Notably, we did not observe changes in the expression of type 1 IFNs in B cells of SLE patients nor a difference in IFN expression in B cells or other PBMC subsets prior and post CD19 CAR T cell therapy (data not shown). These observations suggest that although B cells are (direct or indirect) triggers of the IFN signature in PBMCs, they do not act as the direct source of type 1 IFNs themselves. A likely explanation is that B cell-derived autoantibodies and/or autoantibody-containing immune-complexes trigger IFN expression in tissue resident immune cells, which consequently provokes the IFN response observed in PBMCs of SLE patients. Candidate cells that produce type 1 IFNs in SLE include different dendritic cell subsets such as plasmacytoid dendritic cells as well as tissue macrophages that can produce large amounts of type 1 IFNs in response to toll like receptor activation triggered by immune complexes that contain endogenous nucleic acids (20).
Our current data help to shed light on both the role of B cells as well as on the cascade of events that results from B cell activation and autoreactivity. They additionally provide a rationale to potentially combine and arrange different synergistic preventive and therapeutic approaches such as block of IFN signaling and B cell depletion in order to allow an efficient and rapid suppression of inflammation and enabling a reset autoimmunity, respectively.

Author contributions

GK, GS, DM and AM designed the study and wrote the manuscript. AW, DC and TW designed the study, analyzed data and performed experiments. FM, AB an RGB wrote the manuscript and provided input.

Acknowledgments

This work was funded by the European Union (Horizon 2020 ERC-2020-CoG 101001866 - INSPIRE to G.K. and Horizon 2020 ERC-2018-SyG nanoSCOPE to G.S.).

Conflict of Interest statement

The authors declare no conflict of interest.

References

1. Tsokos GC, Lo MS, Costa Reis P, and Sullivan KE. New insights into the immunopathogenesis of systemic lupus erythematosus. *Nat Rev Rheumatol.* 2016;12(12):716-30.
2. Pisetsky DS, and Lipsky PE. New insights into the role of antinuclear antibodies in systemic lupus erythematosus. *Nat Rev Rheumatol.* 2020;16(10):565-79.
3. Dörner T, Giesecke C, and Lipsky PE. Mechanisms of B cell autoimmunity in SLE. *Arthritis Res Ther.* 2011;13(5):243.
4. Baechler EC, Batliwalla FM, Karypis G, Gaffney PM, Ortmann WA, Espe KJ, et al. Interferon-inducible gene expression signature in peripheral blood cells of patients with severe lupus. *Proc Natl Acad Sci U S A.* 2003;100(5):2610-5.
5. Postal M, Vivaldo JF, Fernandez-Ruiz R, Paredes JL, Appenzeller S, and Niewold TB. Type I interferon in the pathogenesis of systemic lupus erythematosus. *Curr Opin Immunol.* 2020;67:87-94.
6. Vinuesa CG, Shen N, and Ware T. Genetics of SLE: mechanistic insights from monogenic disease and disease-associated variants. *Nat Rev Nephrol.* 2023.
7. Kretschmer S, and Lee-Kirsch MA. Type I interferon-mediated autoinflammation and autoimmunity. *Curr Opin Immunol.* 2017;49:96-102.
8. Wandl UB, Nagel-Hiemke M, May D, Kreuzfelder E, Kloke O, Kranzhoff M, et al. Lupus-like autoimmune disease induced by interferon therapy for myeloproliferative disorders. *Clin Immunol Immunopathol.* 1992;65(1):70-4.
9. Morand EF, Furie R, Tanaka Y, Bruce IN, Askanase AD, Richez C, et al. Trial of Anifrolumab in Active Systemic Lupus Erythematosus. *N Engl J Med.* 2020;382(3):211-21.
10. Merrill JT, Neuwelt CM, Wallace DJ, Shanahan JC, Latinis KM, Oates JC, et al. Efficacy and safety of rituximab in moderately-to-severely active systemic lupus erythematosus: the randomized, double-blind, phase II/III systemic lupus erythematosus evaluation of rituximab trial. *Arthritis Rheum.* 2010;62(1):222-33.
11. Kamburova EG, Koenen HJ, Borgman KJ, ten Berge IJ, Joosten I, and Hilbrands LB. A single dose of rituximab does not deplete B cells in secondary lymphoid organs but alters phenotype and function. *Am J Transplant.* 2013;13(6):1503-11.
12. Frigault MJ, and Maus MV. State of the art in CAR T cell therapy for CD19+ B cell malignancies. *J Clin Invest.* 2020;130(4):1586-94.
13. Mougiakakos D, Kronke G, Volkl S, Kretschmann S, Aigner M, Kharboutli S, et al. CD19-Targeted CAR T Cells in Refractory Systemic Lupus Erythematosus. *N Engl J Med.* 2021;385(6):567-9.
14. Mackensen A, Muller F, Mougiakakos D, Boltz S, Wilhelm A, Aigner M, et al. Anti-CD19 CAR T cell therapy for refractory systemic lupus erythematosus. *Nat Med.* 2022;28(10):2124-32.
15. Muller F, Boeltz S, Knitza J, Aigner M, Volkl S, Kharboutli S, et al. CD19-targeted CAR T cells in refractory antisynthetase syndrome. *Lancet.* 2023;401(10379):815-8.
16. Müller F, Taubmann J, Bucci L, Wilhelm A, Bergmann C, Völkl S, et al. CD19 CAR T-Cell Therapy in Autoimmune Disease - A Case Series with Follow-up. *N Engl J Med.* 2024;390(8):687-700.
17. Crow MK. Pathogenesis of systemic lupus erythematosus: risks, mechanisms and therapeutic targets. *Ann Rheum Dis.* 2023;82(8):999-1014.

18. Leandro MJ, Cambridge G, Ehrenstein MR, and Edwards JC. Reconstitution of peripheral blood B cells after depletion with rituximab in patients with rheumatoid arthritis. *Arthritis Rheum.* 2006;54(2):613-20.
19. Rehnberg M, Amu S, Tarkowski A, Bokarewa MI, and Brisslert M. Short- and long-term effects of anti-CD20 treatment on B cell ontogeny in bone marrow of patients with rheumatoid arthritis. *Arthritis Res Ther.* 2009;11(4):R123.
20. Fillatreau S, Manfroi B, and Dörner T. Toll-like receptor signalling in B cells during systemic lupus erythematosus. *Nat Rev Rheumatol.* 2021;17(2):98-108.
21. Hao Y, Hao S, Andersen-Nissen E, Mauck WM, 3rd, Zheng S, Butler A, et al. Integrated analysis of multimodal single-cell data. *Cell.* 2021;184(13):3573-87.e29.

Figure legends

Figure 1: ScRNAseq-based analysis of PBMCs of SLE Patients.

(A-G) Single cell RNA sequencing (scRNAseq)-based analysis of peripheral blood mononuclear cells (PBMCs) of SLE patients (n=7) before CD19 CAR T cell therapy and after early B cell repopulation. Single datasets from each patient were integrated using the Seurat pipeline into one dataset containing ~ 40.700 PBMCs. **(A)** Dimensional reduction of PBMCs revealing indicated UMAP clusters where cluster identities were determined through top cluster gene analysis and the Enrichr package. **(B,C)** Comparison of single cell datasets from SLE patient before anti-CD19 CAR T cell therapy and after early B cell reconstitution, respectively. **(D)** Differential gene expression analysis on the effect of anti-CD19 CAR T cell therapy. **(E)** Pathway enrichment analysis based on changes in gene expression of total PBMCs. The color intensity reflects the adjusted p-value for each pathway. **(F)** Interferon associated genes are highlighted in a normalized heatmap representing mean gene expression of interferon related genes (n=15 unique genes) before and after CD19 CAR T cell treatment. **(G)** Gene expression levels of *ISG15* and *IRF7* as representative interferon-induced genes are highlighted as feature plot and in violin plots illustrating expression levels on basis of individual patients.

Figure 2: CD19 CAR T Cell-mediated changes in T cell signature and TCR repertoire.

(A-C) ScRNAseq-based re-clustering and visualization of $CD4^+$ and $CD8^+$ T cells pre- and post CD19 CAR T cell treatment using dimensionality reduction on a 2D scale in a UMAP plot. **(D)** Volcano plot and **(E)** pathway enrichment analysis showing the effect of CD19 CAR T cell treatment on the differential gene expression. **(F)** Heatmap displaying changes of interferon-

dependent genes upon CD19 CAR T cell treatment **(G)** ScRNAseq-based T cell receptor repertoire analysis showing V gene usage of TCRß chains and probability of TCR chain generation based on calculation with the OLGA algorithm. Statistical analyses were performed using the median and t-test with Benjamini-Hochberg correction. Significant differences are indicated as follows: *P ≤ 0.05, **P ≤ 0.005, ***P ≤ 0.001, ****P ≤ 0.0001.

Figure 3: CD19 CAR T Cell-mediated changes in B cell signature.

(A-F) ScRNAseq-based analysis of datasets generated from sorted B cells pre and post CD19 CAR T cell therapy illustrated as grouped individual UMAP plots **(A and C)** and calculated relative cell number of indicated B cell subsets **(B)**. Differential gene expression **(D)**, gene expression-based pathway analysis **(E)** and expression of BCR and FcγR signaling related genes **(F)** in scRNAseq datasets derived from isolated B cells pre and post CD19 CAR T cell therapy.

Figure 4: CD19 CAR T Cell-mediated changes in B cell repertoire.

(A) BCR repertoire analysis demonstrating prevalence of Ig subclass distribution following CD19 CAR T cell treatment and the probability of generation of BCRs as calculated by the OLGA algorithm. **(B)** Comparison of expanded clones based on VDJ gene annotation before and after CD19 CAR T cell treatment. **(C)** Top 10 expanded clone analysis on their sharedness and repertoire proportion. Statistical analyses were performed using the median and t-test with Benjamini-Hochberg correction. Significant differences are indicated as follows: *P ≤ 0.05, **P ≤ 0.005, ***P ≤ 0.001, ****P ≤ 0.0001.

Materials and Methods

LEAD CONTACT

Further information and requests for resources and reagents should be directed to the Lead Contact, Gerhard Krönke (gerhard.kroenke@charite.de).

SEX AS BIOLOGICAL VARIANT

This study included both male and female patients (see Table S1). Although the incidence of SLE is increased in females in comparison to males, we do not consider sex as major biologic variable in terms of the response to CD19 CAR T cell therapy.

MATERIALS AVAILABILITY

This study did not generate new unique reagents.

DATA AND CODE AVAILABILITY

The Single Cell Sequencing dataset generated during this study will be available at GEO Platform (Accession number: GSE263931). Supporting data values associated with the main manuscript and supplement material are available as Excel (XLS) file.

STUDY PARTICIPANT DETAILS

Peripheral blood samples were collected from donors before CD19 CAR T Cell therapy as well as after repopulation of B cells after obtaining informed consent in accordance with the CARE guidelines and approval from the Institutional Review Board of the University Clinic of Erlangen under the license 334_18 B. The donor demographic information is provided in Table S1. Peripheral blood mononuclear cells (PBMCs) were isolated by using SepMate™-50 (StemCell) and Ficoll-Paque gradient centrifugation according to manufactures protocol. The isolated PBMCs were then washed and resuspended in PBS with 10 mM EDTA (Invitrogen) for single cell RNA sequencing (scRNA-seq) and in MACS buffer (PBS, 2% FCS, 10 mM) for downstream magnetic B cell isolation. B cell isolation was performed using EasySep™ Human B Cell Enrichment Kit (StemCell) according the manufactures protocol.

METHOD DETAILS

Library Preparation for single cell sequencing

For scRNA-seq and immune repertoire analysis, we employed the Chromium Next GEM Single cell 5´Reagent Kits v2 (10 X Genomics) to generate single-cell cDNA libraries from isolated PBMCs. To increase the yield for B cells we performed cDNA library generation on isolated B cells. The isolated PBMCs and B cells were encapsulated into droplets, and reverse transcription of RNA was performed to generate barcoded cDNA molecules. The final libraries were then sequenced on an Illumina NovaSeq sequencer with 150 base pair long paired-end reads. B cell receptor (BCR) and T cell receptor (TCR) regions were amplified through PCR (polymerase chain reaction) using locus-specific primers targeting constant regions of the respective TCR or BCR. The amplification products were then subjected to high-throughput sequencing on an Illumina NovaSeq platform with 150 base pair long paired-end reads aiming at an average of 15000 mean number of reads per cell. Reads were converted to FASTQ format using mkfastq from Cell Ranger 7.0.0 (10x Genomics).

Single cell sequencing data analysis

The raw scRNA-seq data were preprocessed and analyzed using the Cellranger multi pipeline (v.7.0.0). The reads were mapped to the human reference genome (GRCh38-2020-A). Cell filtering, barcode counting, and UMI (unique molecular identifier) counting and downstream data handling were performed using the Seurat R package (v.4.3) to obtain the count matrices for each individual cell. To filter out low-quality cells, cells with we applied appropriate thresholds for unique molecular identifiers (UMIs), number of detected genes and number of UMIs assigned to mitochondrial genes. All single patient datasets were integrated into one object for global analysis. We performed dimensionality reduction using Principal Component Analysis (PCA) and cell clustering. The number of PCs to be used for clustering was

identified using the ElbowPlot function and clustering resolution was decided on with the clustree R package (v.0.5.0). Cluster identity was determined using the EnrichR R package (v3.2) as well as common marker expression. T cells and B cells were identified using common marker expression of CD3, CD4, CD8 and CD19 respectively. Subsequently T cells and B cells were filtered, selected for cells that have a sequenced TCR or BCR and re-clustered separately (21).

BCR and TCR Sequencing

Clonotype calling was performed using the Cellranger multi pipeline (v.7.0.0). Integration of the BCR/TCR data was done with the Seurat R package (v.4.3) and TCR/BCR diversity and clonality analysis was performed using the scRepertoire R package (v.1.10.0)

Differential Expression and Pathway Analysis

Differentially expressed genes (DEGs) for all sets of cells were determined using the FindAllMarkers function of the Seurat package using the default settings. The identified DEGs were then used as input for Pathway Enrichment Analysis (PEA) with the pathfinder R package (v.1.6.4). The Reactome pathway database was used as a reference for pathway specific gene sets.

CDR3 region generation probability estimation

To estimate the likelihood of BCR and TCR CDR3 sequence generation, we utilized the Optimized Likelihood estimate of immunoGlobulin Amino-acid sequences (OLGA) tool (v.1.2.4). Cell that are not compatible with any recombination scenario were filtered out.

QUANTIFICATION AND STATISTICAL ANALYSIS

Statistical analysis was carried out in R and a complete description is available in the associated figure legends. For generating figures we used the R packages ggplot2 (v.3.4.2), scRepertoire (v1.7.2), EnhancedVolcano (v.1.14.0), ComplexHeatmap (v.2.16.0) and pheatmap (v.1.0.12) as well as Adobe Illustrator CC 2018 (v.22.1).

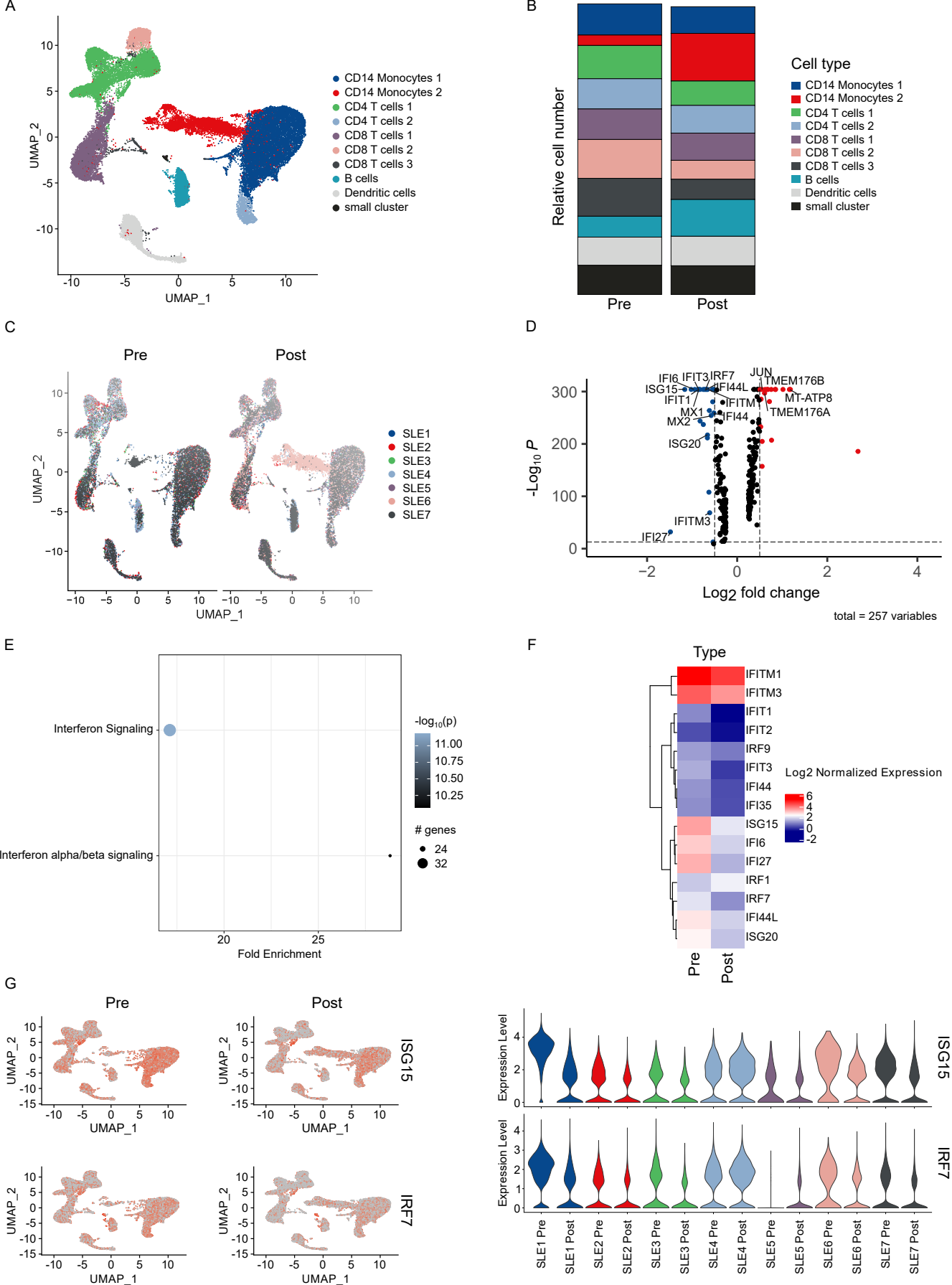
A
UMAP_2
UMAP_1
CD14 Monocytes 1
CD14 Monocytes 2
CD4 T cells 1
CD4 T cells 2
CD8 T cells 1
CD8 T cells 2
CD8 T cells 3
B cells
Dendritic cells
small cluster
B
Relative cell number
Pre
Post
Cell type
C
Pre
Post
UMAP_2
UMAP_1
SLE1
SLE2
SLE3
SLE4
SLE5
SLE6
SLE7
D
-Log10 P
Log2 fold change
total = 257 variables
IFI6
IFIT3
IRF7
JUN
TMEM176B
ISG15
IFI44L
MT-ATP8
IFIT1
IFITM1
TMEM176A
MX1
MX2
IFI44
ISG20
IFITM3
IFI27
E
Interferon Signaling
Interferon alpha/beta signaling
-log10(p)
11.00
10.75
10.50
10.25
genes
24
32
Fold Enrichment
F
Type
IFITM1
IFITM3
IFIT1
IFIT2
IRF9
IFIT3
IFI44
IFI35
ISG15
IFI6
IFI27
IRF1
IRF7
IFI44L
ISG20
Log2 Normalized Expression
Pre
Post
G
Pre
Post
ISG15
IRF7
UMAP_2
UMAP_1
Expression Level
SLE1 Pre
SLE1 Post
SLE2 Pre
SLE2 Post
SLE3 Pre
SLE3 Post
SLE4 Pre
SLE4 Post
SLE5 Pre
SLE5 Post
SLE6 Pre
SLE6 Post
SLE7 Pre
SLE7 Post

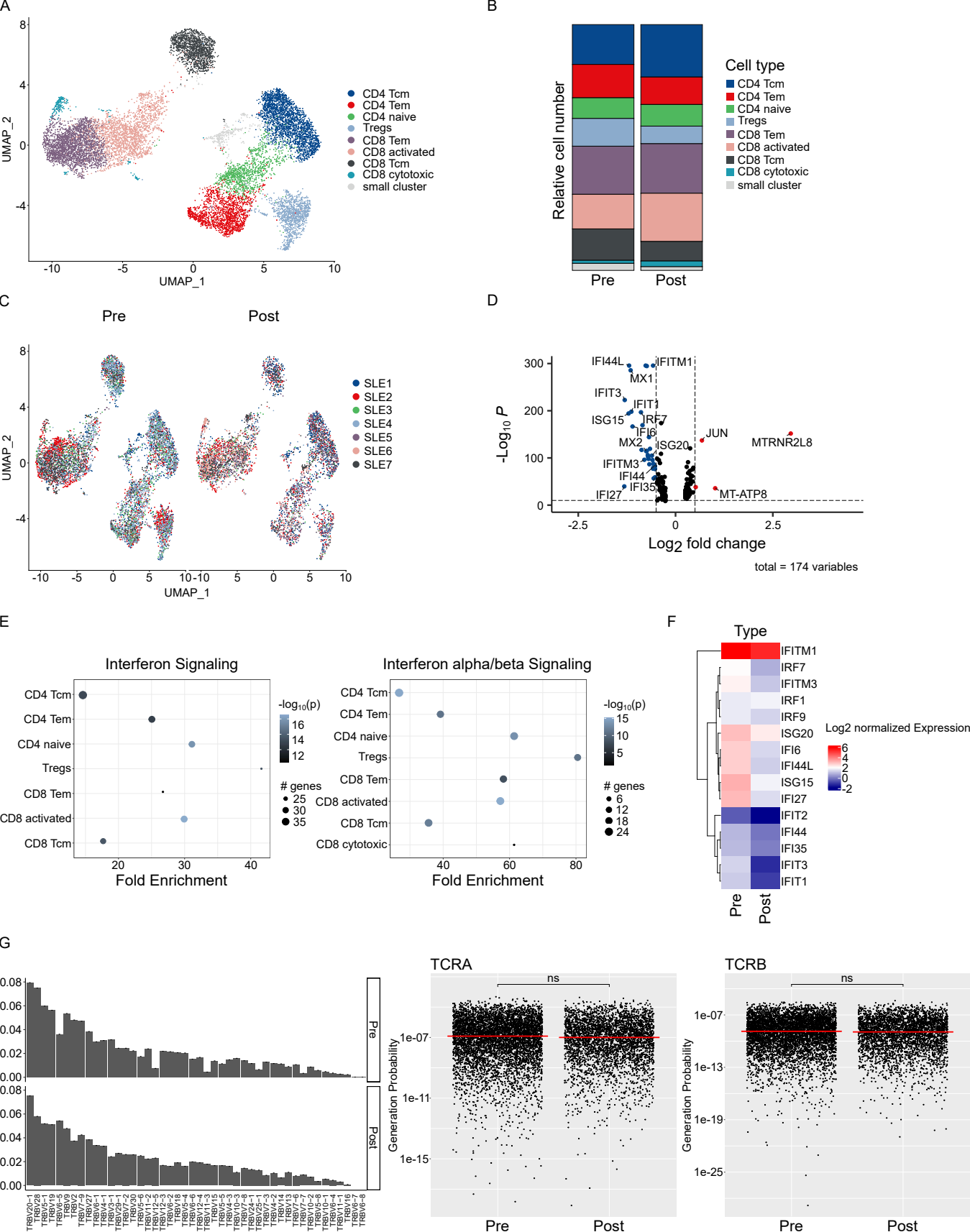
A
UMAP_2
UMAP_1
CD4 Tcm
CD4 Tem
CD4 naive
Tregs
CD8 Tem
CD8 activated
CD8 Tcm
CD8 cytotoxic
small cluster
B
Relative cell number
Cell type
Pre
Post
C
Pre
Post
SLE1
SLE2
SLE3
SLE4
SLE5
SLE6
SLE7
D
-Log10 P
Log2 fold change
total = 174 variables
IFI44L
IFITM1
MX1
IFIT3
IFIT1
ISG15
IRF7
IFI6
MX2
ISG20
JUN
MTRNR2L8
IFITM3
IFI44
IFI35
IFI27
MT-ATP8
E
Interferon Signaling
Interferon alpha/beta Signaling
-log10(p)
genes
Fold Enrichment
F
Type
Log2 normalized Expression
IFITM1
IRF7
IFITM3
IRF1
IRF9
ISG20
IFI6
IFI44L
ISG15
IFI27
IFIT2
IFI44
IFI35
IFIT3
IFIT1
Pre
Post
G
Pre
Post
TCRA
TCRB
ns
Generation Probability
Pre
Post

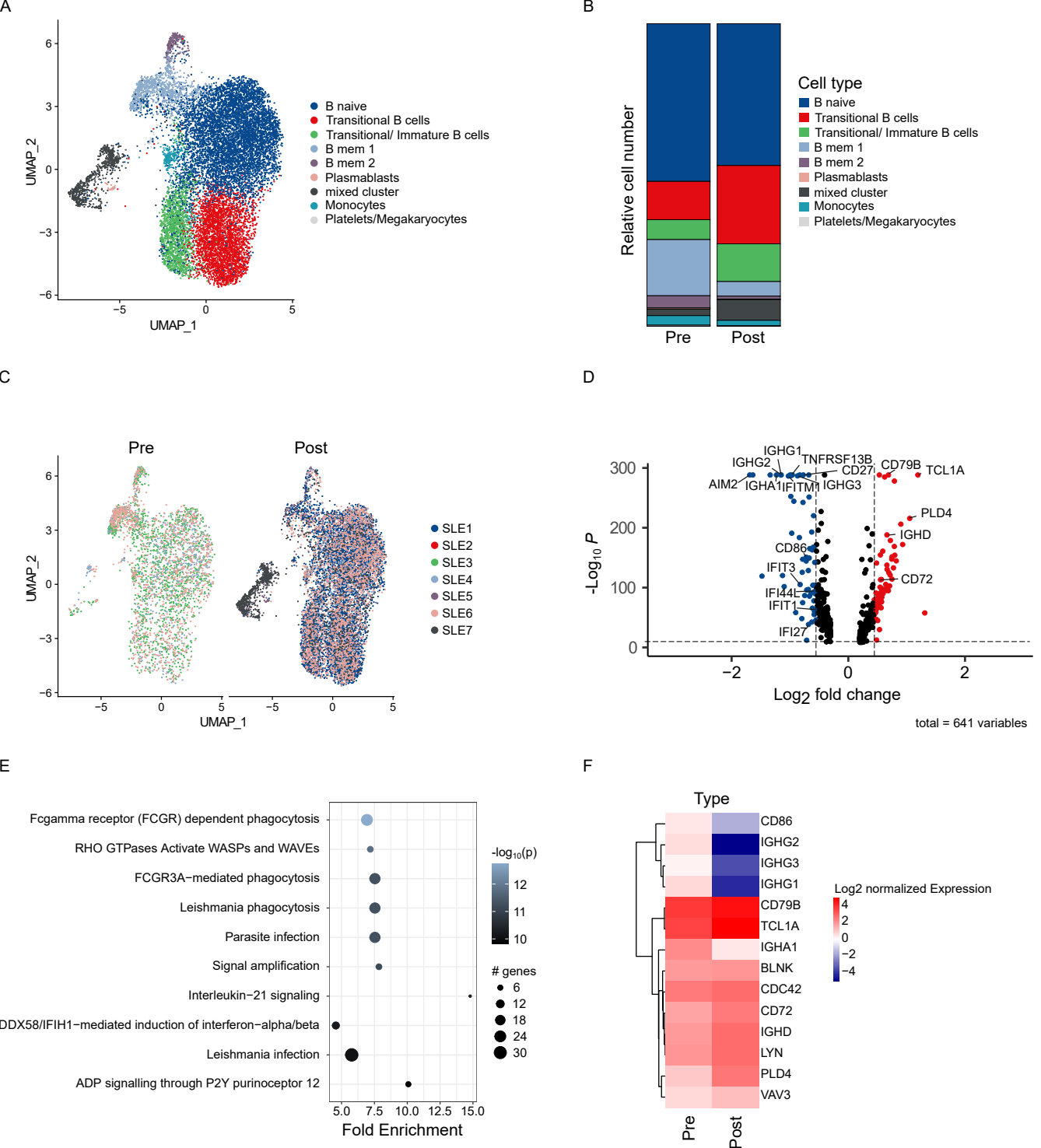
A
UMAP_2
UMAP_1
B naive
Transitional B cells
Transitional/ Immature B cells
B mem 1
B mem 2
Plasmablasts
mixed cluster
Monocytes
Platelets/Megakaryocytes
B
Relative cell number
Cell type
Pre
Post
C
Pre
Post
SLE1
SLE2
SLE3
SLE4
SLE5
SLE6
SLE7
D
-Log10 P
Log2 fold change
total = 641 variables
IGHG1
IGHG2
TNFRSF13B
CD27
CD79B
TCL1A
AIM2
IGHA1
IFITM1
IGHG3
PLD4
IGHD
CD86
IFIT3
CD72
IFI44L
IFIT1
IFI27
E
Fcgamma receptor (FCGR) dependent phagocytosis
RHO GTPases Activate WASPs and WAVEs
FCGR3A−mediated phagocytosis
Leishmania phagocytosis
Parasite infection
Signal amplification
Interleukin−21 signaling
DDX58/IFIH1−mediated induction of interferon−alpha/beta
Leishmania infection
ADP signalling through P2Y purinoceptor 12
-log10(p)
genes
Fold Enrichment
F
Type
CD86
IGHG2
IGHG3
IGHG1
CD79B
TCL1A
IGHA1
BLNK
CDC42
CD72
IGHD
LYN
PLD4
VAV3
Log2 normalized Expression
Pre
Post

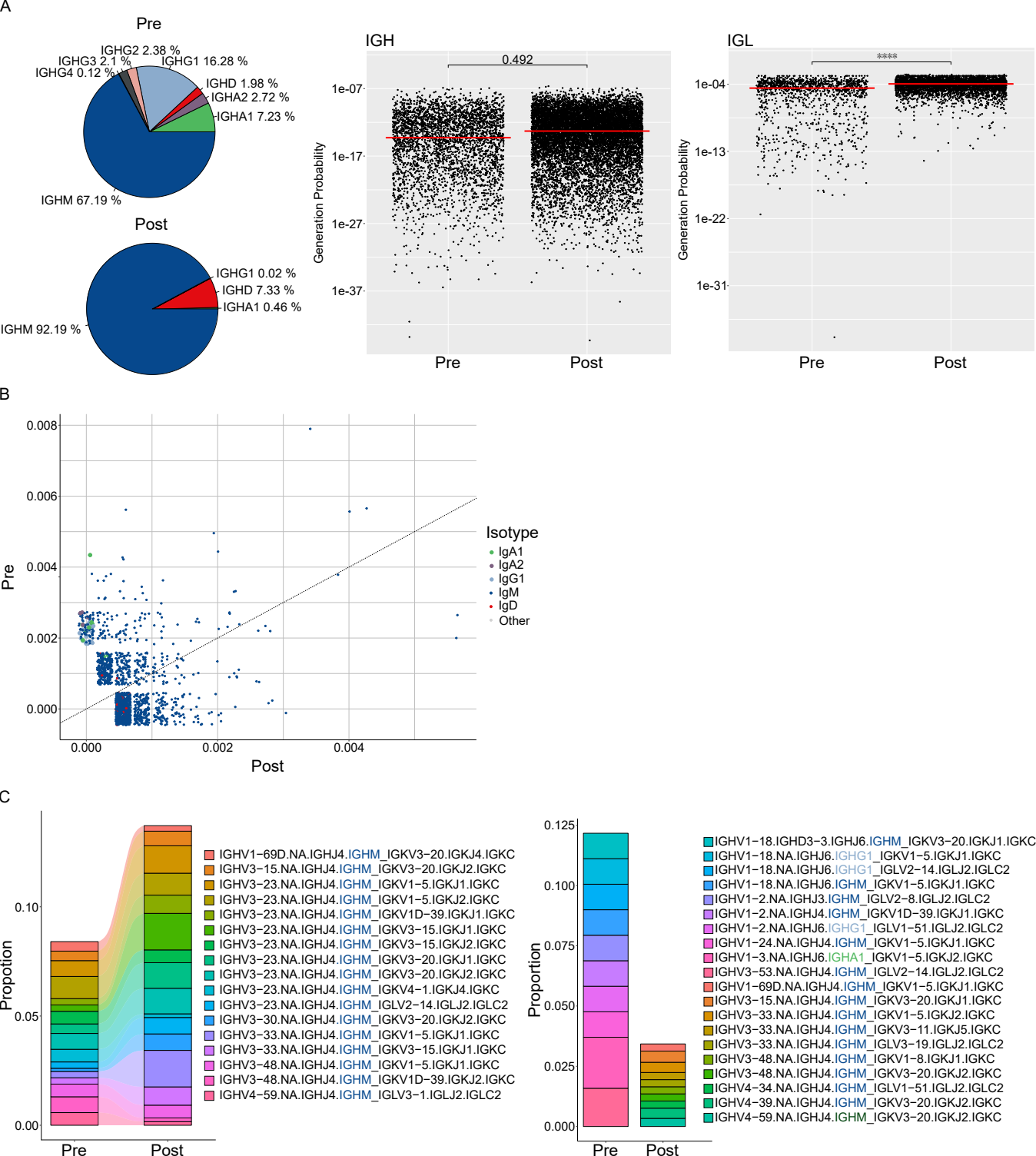
A
Pre
IGHG2 2.38 %
IGHG3 2.1 %
IGHG1 16.28 %
IGHG4 0.12 %
IGHD 1.98 %
IGHA2 2.72 %
IGHA1 7.23 %
IGHM 67.19 %
Post
IGHG1 0.02 %
IGHD 7.33 %
IGHA1 0.46 %
IGHM 92.19 %
IGH
0.492
Generation Probability
1e-07
1e-17
1e-27
1e-37
Pre
Post
IGL
****
Generation Probability
1e-04
1e-13
1e-22
1e-31
Pre
Post
B
Pre
Post
0.008
0.006
0.004
0.002
0.000
Isotype
IgA1
IgA2
IgG1
IgM
IgD
Other
C
Propotion
0.10
0.05
0.00
Pre
Post
IGHV1−69D.NA.IGHJ4.IGHM_IGKV3−20.IGKJ4.IGKC
IGHV3−15.NA.IGHJ4.IGHM_IGKV3−20.IGKJ2.IGKC
IGHV3−23.NA.IGHJ4.IGHM_IGKV1−5.IGKJ1.IGKC
IGHV3−23.NA.IGHJ4.IGHM_IGKV1−5.IGKJ2.IGKC
IGHV3−23.NA.IGHJ4.IGHM_IGKV1D−39.IGKJ1.IGKC
IGHV3−23.NA.IGHJ4.IGHM_IGKV3−15.IGKJ1.IGKC
IGHV3−23.NA.IGHJ4.IGHM_IGKV3−15.IGKJ2.IGKC
IGHV3−23.NA.IGHJ4.IGHM_IGKV3−20.IGKJ1.IGKC
IGHV3−23.NA.IGHJ4.IGHM_IGKV3−20.IGKJ2.IGKC
IGHV3−23.NA.IGHJ4.IGHM_IGKV4−1.IGKJ4.IGKC
IGHV3−23.NA.IGHJ4.IGHM_IGLV2−14.IGLJ2.IGLC2
IGHV3−30.NA.IGHJ4.IGHM_IGKV3−20.IGKJ2.IGKC
IGHV3−33.NA.IGHJ4.IGHM_IGKV1−5.IGKJ1.IGKC
IGHV3−33.NA.IGHJ4.IGHM_IGKV3−15.IGKJ1.IGKC
IGHV3−48.NA.IGHJ4.IGHM_IGKV1−5.IGKJ1.IGKC
IGHV3−48.NA.IGHJ4.IGHM_IGKV1D−39.IGKJ2.IGKC
IGHV4−59.NA.IGHJ4.IGHM_IGLV3−1.IGLJ2.IGLC2
Proportion
0.125
0.100
0.075
0.050
0.025
0.000
Pre
Post
IGHV1−18.IGHD3−3.IGHJ6.IGHM_IGKV3−20.IGKJ1.IGKC
IGHV1−18.NA.IGHJ6.IGHG1_IGKV1−5.IGKJ1.IGKC
IGHV1−18.NA.IGHJ6.IGHG1_IGLV2−14.IGLJ2.IGLC2
IGHV1−18.NA.IGHJ6.IGHM_IGKV1−5.IGKJ1.IGKC
IGHV1−2.NA.IGHJ3.IGHM_IGLV2−8.IGLJ2.IGLC2
IGHV1−2.NA.IGHJ4.IGHM_IGKV1D−39.IGKJ1.IGKC
IGHV1−2.NA.IGHJ6.IGHG1_IGLV1−51.IGLJ2.IGLC2
IGHV1−24.NA.IGHJ4.IGHM_IGKV1−5.IGKJ1.IGKC
IGHV1−3.NA.IGHJ6.IGHA1_IGKV1−5.IGKJ2.IGKC
IGHV3−53.NA.IGHJ4.IGHM_IGLV2−14.IGLJ2.IGLC2
IGHV1−69D.NA.IGHJ4.IGHM_IGKV1−5.IGKJ1.IGKC
IGHV3−15.NA.IGHJ4.IGHM_IGKV3−20.IGKJ1.IGKC
IGHV3−33.NA.IGHJ4.IGHM_IGKV1−5.IGKJ2.IGKC
IGHV3−33.NA.IGHJ4.IGHM_IGKV3−11.IGKJ5.IGKC
IGHV3−33.NA.IGHJ4.IGHM_IGLV3−19.IGLJ2.IGLC2
IGHV3−48.NA.IGHJ4.IGHM_IGKV1−8.IGKJ1.IGKC
IGHV3−48.NA.IGHJ4.IGHM_IGKV3−20.IGKJ2.IGKC
IGHV4−34.NA.IGHJ4.IGHM_IGLV1−51.IGLJ2.IGLC2
IGHV4−39.NA.IGHJ4.IGHM_IGKV3−20.IGKJ2.IGKC
IGHV4−59.NA.IGHJ4.IGHM_IGKV3−20.IGKJ2.IGKC

ID	Sex	Age*	Disease
SLE1	Female	20	SLE
SLE2	Male	22	SLE
SLE3	Female	22	SLE
SLE4	Female	24	SLE/nephrotic snydrom
SLE5	Female	18	SLE
SLE6	Female	38	SLE
SLE7	Female	33	SLE

* at time of CD19 CAR T cell application

Table S1. Summary of patient information treated with CD19 CAR T cells. Sample identifiers related to Figures 1-3.

ID	CAR T cell application	Time point pre therapy	B cells/µL	Time point post therapy	B cells/µL
SLE1	22.03.2021	17.03.2021	19	21.10.2021	148
SLE2	09.08.2021	04.08.2021	85	30.03.2022	108
SLE3	13.12.2021	23.11.2021	177	11.05.2021	23
SLE4	20.12.2021	06.12.2021	280	11.05.2021	853
SLE5	07.02.2022	25.01.2022	234	08.06.2022	15
SLE6	09.05.2022	25.04.2022	1	06.12.2022	93
SLE7	26.09.2022	20.09.2022	25	05.12.2022	282

Table S2. Summary of time points for the effect CD19 CAR T cells treatment analysis. Sample identifiers related to Figures 1-3.